

## Structural Design of Anthraquinone Bridges in Direct Electron Transfer of Fructose Dehydrogenase

Jansen, Charlotte Uldahl; Yan, Xiaomei; Ulstrup, Jens; Xiao, Xinxin; Qvortrup, Katrine

*Published in:*  
Colloids and Surfaces B: Biointerfaces

*DOI (link to publication from Publisher):*  
[10.1016/j.colsurfb.2022.112941](https://doi.org/10.1016/j.colsurfb.2022.112941)

*Creative Commons License*  
CC BY 4.0

*Publication date:*  
2022

*Document Version*  
Publisher's PDF, also known as Version of record

[Link to publication from Aalborg University](#)

*Citation for published version (APA):*

Jansen, C. U., Yan, X., Ulstrup, J., Xiao, X., & Qvortrup, K. (2022). Structural Design of Anthraquinone Bridges in Direct Electron Transfer of Fructose Dehydrogenase. *Colloids and Surfaces B: Biointerfaces*, 220, Article 112941. <https://doi.org/10.1016/j.colsurfb.2022.112941>

### General rights

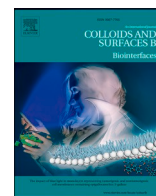
Copyright and moral rights for the publications made accessible in the public portal are retained by the authors and/or other copyright owners and it is a condition of accessing publications that users recognise and abide by the legal requirements associated with these rights.

- Users may download and print one copy of any publication from the public portal for the purpose of private study or research.
- You may not further distribute the material or use it for any profit-making activity or commercial gain
- You may freely distribute the URL identifying the publication in the public portal -

### Take down policy

If you believe that this document breaches copyright please contact us at [vbn@aub.aau.dk](mailto:vbn@aub.aau.dk) providing details, and we will remove access to the work immediately and investigate your claim.





# Structural design of anthraquinone bridges in direct electron transfer of fructose dehydrogenase

Charlotte Uldahl Jansen<sup>a</sup>, Xiaomei Yan<sup>a</sup>, Jens Ulstrup<sup>a</sup>, Xinxin Xiao<sup>a,b,\*</sup>, Katrine Qvortrup<sup>a,\*\*</sup>

<sup>a</sup> Department of Chemistry, Technical University of Denmark, Kongens Lyngby 2800, Denmark

<sup>b</sup> Department of Chemistry and Bioscience, Aalborg University, 9220 Aalborg, Denmark

## ARTICLE INFO

### Keywords:

Anthraquinone  
Fructose dehydrogenase  
Enzyme orientation  
Direct electron transfer  
Bio-interface

## ABSTRACT

Multi-functional small molecules attached to an electrode surface can bind non-covalently to the redox enzyme fructose dehydrogenase (FDH) to ensure efficient electrochemical electron transfer (ET) and electrocatalysis of the enzyme in both mediated (MET) and direct (DET) ET modes. The present work investigates the potential of exploiting secondary, electrostatic and hydrophobic interactions between substituents on a small molecular bridge and the local FDH surfaces. Such interactions ensure alignment of the enzyme in an orientation favourable for both MET and DET. We have used a group of novel synthesized anthraquinones as the small molecule bridge, functionalised with electrostatically neutral, anionic, or cationic substituents. Particularly, we investigated the immobilisation of FDH on a nanoporous gold (NPG) electrode decorated with the novel synthesised anthraquinones using electrochemical methods. The best DET-capable fraction out of four anthraquinone derivatives tested is achieved for an anthraquinone functionalised with an anionic sulphonate group. Our study demonstrates, how the combination of chemical design and bioelectrochemistry can be brought to control alignment of enzymes in productive orientations on electrodes, a paradigm for thiol modified surfaces in biosensors and bioelectronics.

## 1. Introduction

Enzyme immobilisation on electrodes, allowing for controlled electron transfer (ET), is of crucial importance for multiple purposes. These include both fundamental understanding of interfacial ET mechanisms [1, 2] and a variety of biochemical applications [3–5], e.g. in biosensors [6–7] and biofuel cells [1,4,8]. Immobilisation prevents diffusion of the enzyme from the electrode surface into the solution, increasing the overall catalytic efficiency [1,7]. Immobilization also improves enzyme stability [2,7] by protecting the enzymes against temperature, solvent effects, and pH [9]. In addition, in industrial processes, enzyme immobilisation can simplify the downstream processing by streamlining separation and reusing enzymes, and overall enhancing enzyme stability both under storage and operational conditions [4,9].

There are two types of processes in bioelectrochemical ET, i.e., mediated ET (MET) and direct ET (DET) [3]. In MET, redox mediators

shuttle electrons between the enzyme redox centres and the electrode surface [3], while in DET electrons tunnel directly between the enzyme and the electrode [10,11]. To achieve efficient DET, it is crucial that the enzyme is positioned in the correct orientation [1], i.e., the “electro-active” configuration [4], where the distance from the active centre or an electron transfer relay [2,12] relative to the electrode surface does not exceed about 20 Å and the orientation is right [1, 2,13,14]. There are different methods for improving enzyme orientation on electrodes, mostly relying on surface-modification of the electrode [1,2]. One particular method involves modification of gold electrodes with thiol-functionalised small molecules to form self-assembled molecular monolayers (SAMs) through Au-S bonds [15,16]. The small molecules are designed to bind the enzyme either covalently (via maleimide-thiol chemistry, azide-alkyne cycloaddition, imine formation) or through non-covalent interactions (hydrophobic,  $\pi$ - $\pi$  stacking, electrostatic) [2].

Lalaoui and associates [17] showed that 9,10-anthraquinone (AQ)

**Abbreviations:** AQ, anthraquinone; CV, cyclic voltammetry; DET, direct electron transfer;  $E^0$ , apparent formal potential; ET, electron transfer; FAD, flavin adenine dinucleotide; FDH, fructose dehydrogenase; FT, fructose; MET, mediated electron transfer; NPG, nanoporous gold; SAM, self-assembled monolayer;  $\Delta j$ , electrocatalytic current;  $\chi_{DET\%}$ , DET-capable fraction.

\* Corresponding author at: Department of Chemistry, Technical University of Denmark, Kongens Lyngby 2800, Denmark.

\*\* Corresponding author.

E-mail addresses: [xixiao@kemi.dtu.dk](mailto:xixiao@kemi.dtu.dk) (X. Xiao), [kaqvo@kemi.dtu.dk](mailto:kaqvo@kemi.dtu.dk) (K. Qvortrup).

<https://doi.org/10.1016/j.colsurfb.2022.112941>

Received 1 July 2022; Received in revised form 30 September 2022; Accepted 13 October 2022

Available online 14 October 2022

0927-7765/© 2022 The Author(s). Published by Elsevier B.V. This is an open access article under the CC BY license (<http://creativecommons.org/licenses/by/4.0/>).

binds strongly to the enzyme laccase in a hydrophobic pocket close to the catalytic centre. Inspired by this finding, the current study introduces a class of rationally functionalised anthraquinones suggested to offer an efficient binding mode for the redox enzyme fructose dehydrogenase (FDH), which contains a hydrophobic motif similar to that of laccase [18]. FDH consists of a catalytic centre (flavin adenine dinucleotide (FAD)), in which the redox reaction, oxidation of D-fructose to 5-keto-D-fructose, occurs. Associated heme groups function as electronic relay centres [3,19]. During oxidation of fructose, the FAD group (formal potential ( $E^0$ )  $\approx -0.27$  V vs Ag/AgCl, pH 5.5) accepts two electrons, which are then transported to heme 2c ( $E^0 \approx 0.06$  V vs Ag/AgCl, pH 5.5) via heme 3c ( $E^0 \approx -0.01$  V vs Ag/AgCl, pH 5.5). The potential of heme 1c ( $E^0 \approx 0.15$  V vs Ag/AgCl, pH 5.5) is too high for this unit to participate efficiently in the DET pathway but is believed to hold a structural or other function [3,20], see Scheme 1.

Kawai and associates suggested that small molecular bridges can be designed to allow secondary interactions that orient the enzyme [22] in a favourable position for DET. Our recent work [3] demonstrates the importance of the properties of the FDH binding groups of the molecular bridge (substituents  $R_1$  and  $R_2$  in Scheme 1) for efficient interaction with the enzyme surface. The polar but electrostatically, neutral 2-mercaptoethanol and the negatively charged mercaptopropionic acid both showed high FDH surface coverage and interfacial ET rates. The current study proposes that molecular bridge molecules, rationally designed with suitable functional groups, can be utilized to control proper surface orientation of FDH for DET through chosen secondary interactions with relevant charge distributions on the enzymatic surface around the targeted enzyme hydrophobic motif. To investigate this, a group of four anthraquinones (see Scheme 2) was designed, synthesised, and their ability to interact with the enzyme, as well as their ability to orient the enzyme correctly in relation to the electrode investigated. The four analogues are the electrostatically neutral hydrophobic unsubstituted anthraquinone AQdd (1), 1-amino substituted AQdS (2, primary aniline  $pK_a = 4.6$  [23]), which is likely to interact with anionic surface residues on the enzyme around pH 5, while the 2-sulphonate functionalized anthraquinone (AQdA, 3, benzenesulfonic acid  $pK_a = -2.8$  [24]) could interact with cationic surface residues on the enzyme. An analogue containing both the 1-ammonio and 2-sulphonate substituents (AQSH, 4) and therefore expected to exist as a zwitterion is included in the study as a neutral but polar anthraquinone, Scheme 2.

4) and therefore expected to exist as a zwitterion is included in the study as a neutral but polar anthraquinone, Scheme 2.

## 2. Experimental section

The four AQ analogues were synthesised from the commercially available sodium 1-amino-4-bromo-anthraquinone-2-sulphonate, by first inserting the required thiol handle followed by chemoselective removal of functionalities. Nanoporous gold film (NPG) modified glassy carbon electrodes were grafted with the anthraquinone derivatives to form SAMs, and their DET properties recorded by monitoring the catalytic anodic current via cyclic voltammetry (CV), in the presence of fructose as the enzyme substrate. For general methodologies, experimental procedures, analytical characterisation and electrode preparation, see supporting information.

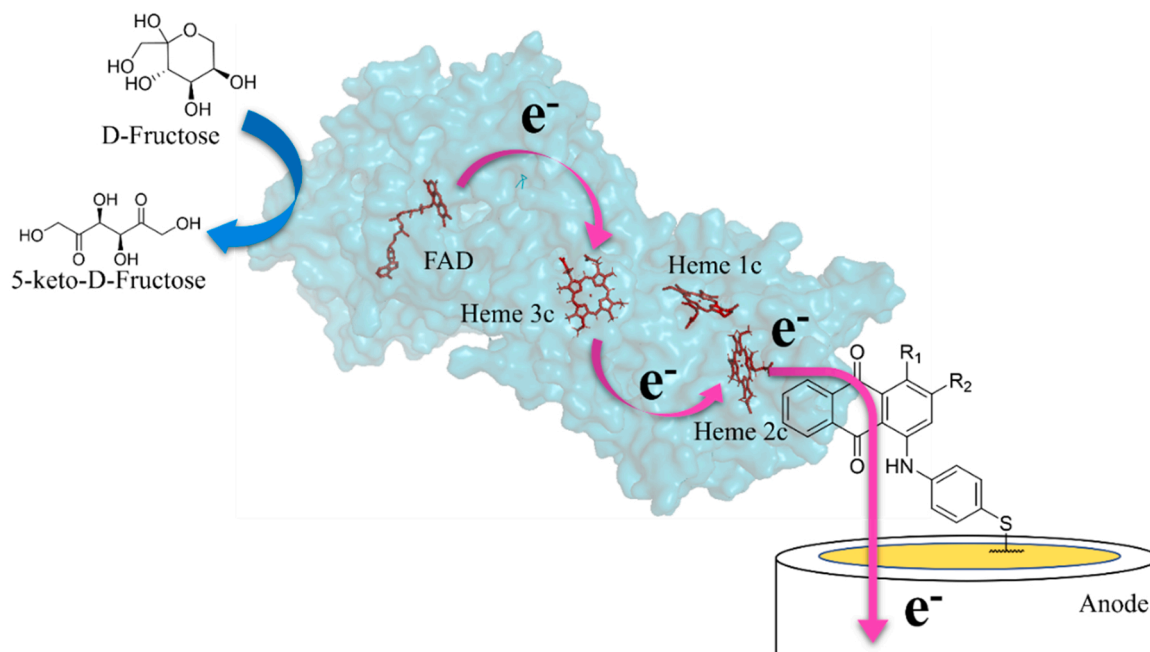
### 2.1. Synthesis strategy

The four AQ analogues were synthesised from the starting material sodium 1-amino-4-bromo-anthraquinone-2-sulphonate (5), starting with a Cu(0)-catalyzed Ullmann condensation [25], with S-(4-amino-phenyl) ethanethioate (6), synthesized from 7 (Scheme 3). The reaction proceeded smoothly in freshly prepared phosphate buffer under microwave heating (120 °C) for 20 min, Scheme 4. This gave the first analogue AQSH (4).

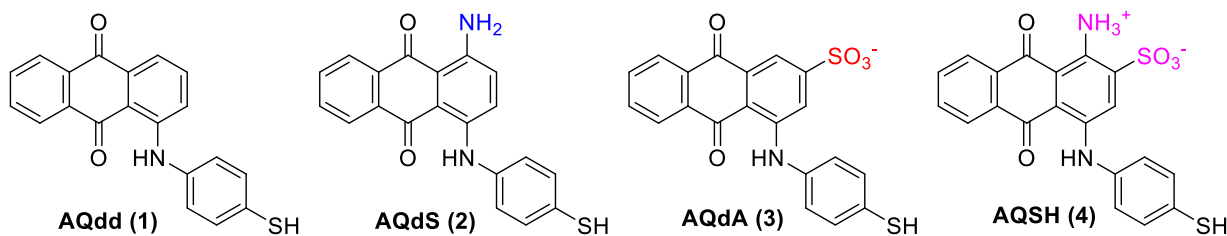
The other three analogues could be synthesised from AQSH (4) by sequential chemoselective removal of the substituents, Scheme 4. The primary aniline was removed through diazotization with sodium nitrite, followed by the addition of zinc powder in ethanol [26], selectively affording the AQdA (3) analogue. The sulphonic acid substituent was removed with glucose and 30 w% sodium hydroxide [27,28] to give the AQdS (2) analogue. The AQdd (1) analogue was synthesised by stepwise removal of each of the substituents as previously described.

### 2.2. Electrode modification

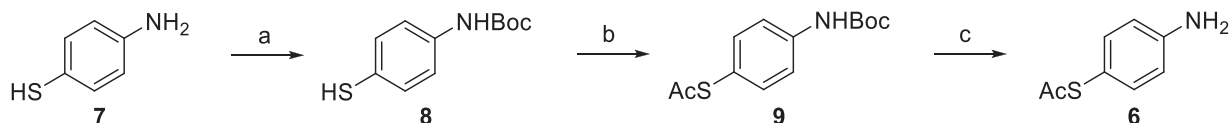
NPG (thickness ca. 100 nm, average pore size 30 nm, roughness factor 7–8) was prepared via a chemical dealloying method [29], used to



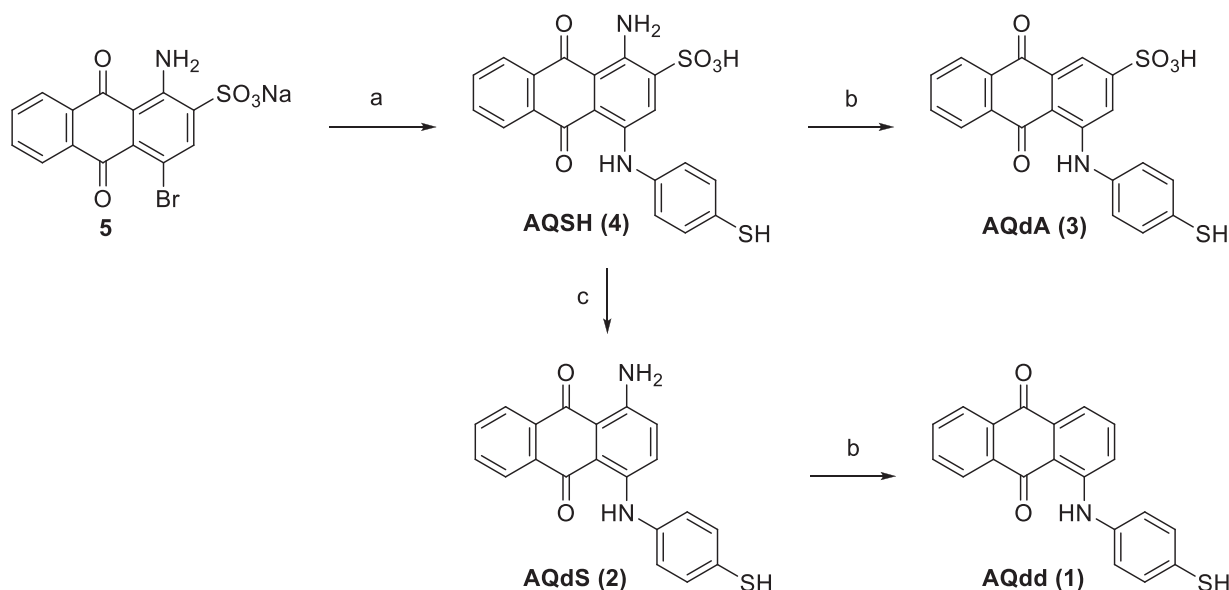
**Scheme 1.** Schematic illustration of FDH in electrochemical reaction on an anodic electrode surface. The ET groups and ET pathways are highlighted (modified from PhD Thesis of Charlotte Uldahl Jansen [21]), homology model adapted with permission from [3].



**Scheme 2.** The four target anthraquinones with different substituent patterns. The primary aniline of AQdS (2) is not protonated at pH 5.5.



**Scheme 3.** Synthetic strategy for S-(4-aminophenyl) ethanethioate (6). a)  $\text{Boc}_2\text{O}$ ,  $\text{H}_2\text{O}$ , room temperature, 24 h. b)  $\text{AcCl}$ ,  $\text{NEt}_3$ ,  $\text{DCM}$ ,  $0^\circ\text{C}$ , 30 min c)  $\text{TFA}$ , room temperature, 30 min.



**Scheme 4.** Synthetic strategy for the four AQ derivatives. a) **6**,  $\text{Cu}(0)$ , phosphate buffer, microwave,  $120^\circ\text{C}$ , 20 min b)  $\text{NaNO}_2$ , 1 M  $\text{HCl}$ ,  $0^\circ\text{C}$ , 20 s; then  $\text{Zn}$ ,  $\text{EtOH}$ . c) glucose, 30 w%  $\text{NaOH}$ ,  $\text{H}_2\text{O}$ ,  $80^\circ\text{C}$ , 30 min.

increase the effective working area of the electrode [30]. The AQ derivatives were grafted to a NPG modified glassy carbon electrode forming Au-S bond based SAMs, by immersing the electrode in an AQ aqueous solution (1–1.5 mM) for 24 hrs. The AQ modified electrode was gently washed with milli-Q water and then immersed in a solution of the enzyme ( $0.6 \text{ mg mL}^{-1}$ , McIlvaine buffer, 100 mM, pH 5.5) for 24 hrs, to attach the enzyme to the AQ functionalised electrode. Details of electrode preparation are given in [supporting information](#).

### 2.3. Electrochemical analysis

CV was used to analyse the electrochemical behaviour of the enzyme AQ-bridged electrodes, which were used as the working electrode in a three-electrode system, with an  $\text{Ag}/\text{AgCl}$  (3 M  $\text{KCl}$ ) reference electrode and a Pt wire-based counter electrode. Ar gas saturated 100 mM pH 5.5 McIlvaine buffer was used as the electrolyte. The background CV was initially recorded without the enzyme substrate (fructose) present, followed by recording the CV in the presence of fructose (100 mM). The MET response was recorded, with the mediator ferrocene-MeOH ( $\text{FcMeOH}$ , 0.5 mM) added to the buffer solution followed by recording of the CV data both with and without fructose present, similarly to the

DET recordings. The CVs are shown in [Fig. 1](#), presented as the apparent current density ( $\mu\text{A cm}^{-2}$ ) against the potential applied (V), normalized to the geometric area of the electrode.

### 3. Results and discussion

The DET CVs ([Fig. 1a, c, e, g](#)) of the enzyme immobilised on the variably functionalised AQ SAMs show a characteristic oxidation peak from the enzyme [10] (red line, with enzyme substrate). Blank curves with enzyme, but no enzyme substrate, are shown by grey lines; no redox peak features are observed here. The onset potentials for oxidising currents of the four bioelectrodes were estimated to be at 0.02 V by comparing the curves in the presence and absence of fructose. This value is close to  $E^0$  of heme 2c of 0.06 V. In the absence of the enzyme substrate (grey line, with  $\text{FcMeOH}$ ), a pair of well-defined redox peaks (midpoint redox potential approximately 0.23 V) of  $\text{FcMeOH}$  are observed for the MET CVs ([Fig. 1b, d, f, h](#)). When the enzyme substrate is present, the oxidation of the enzyme is, however, the major contributor to the CV, with no reductive currents observed. AQdd (1, [Fig. 1h](#)) shows the characteristic sigmoidal shape expected for enzyme MET oxidation, while the shapes of AQSH (4, [Fig. 1b](#)), AQdS (2, [Fig. 1d](#)) and AQdA (3,

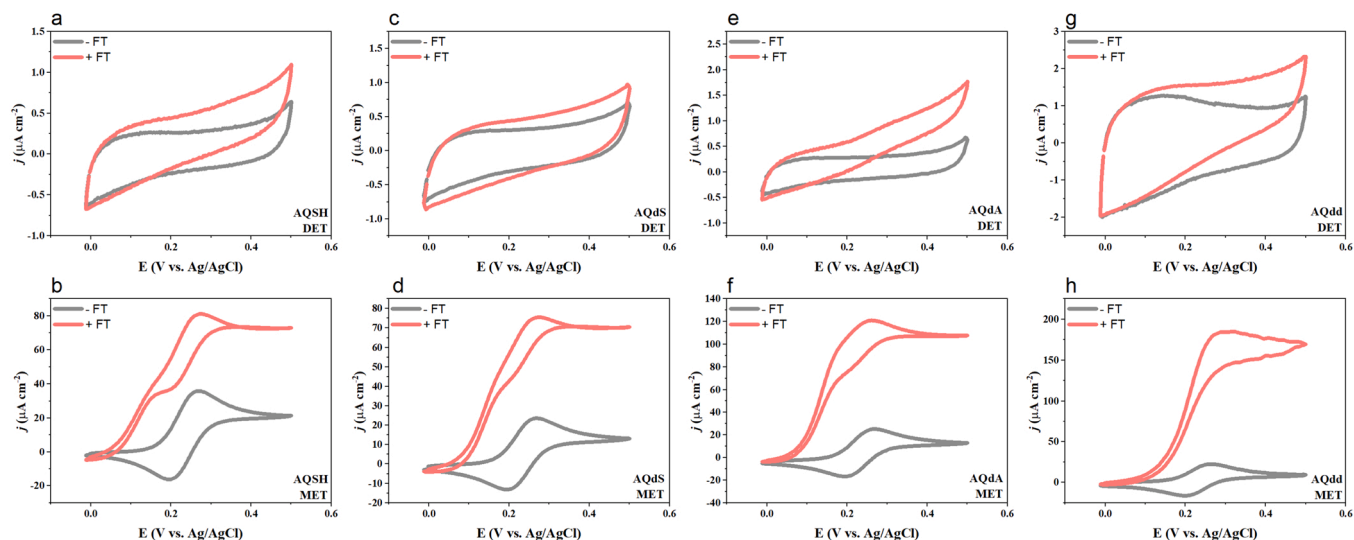


**Fig. 1.** FDH CV data for AQ derivatives at  $5 \text{ mV s}^{-1}$ , depicted as  $j \text{ (}\mu\text{A cm}^{-2}\text{)}$  against  $E \text{ (V vs. Ag/AgCl)}$ . The baseline without enzyme substrate (fructose) is marked as “-FT” (grey) and with 100 mM substrate (fructose) as “+FT” (red). AQSH (4) DET (a) and MET (b), AQdS (2) DET (c) and MET (d), AQdA (3) DET (e) and MET (f), AQdd (1) DET (g) and MET (h).

Fig. 1f) are also affected by the mediator faradaic contribution. This may be due to lower enzyme loading on the working electrode of AQSH (4), AQdS (2) and AQdA (3) compared to that of AQdd (1).

The point 0.5 V was chosen as oxidizing potential for obtaining the anodic catalytic current density, with background current density deducted, when investigating the trends among the different Aqs. The background-corrected electrocatalytic current density ( $\Delta j$ ) at 0.5 V was calculated from the data presented in Fig. 1, using Eq. (1) for DET, and Eq. (2) for MET.

$$\Delta j_{\text{DET}} = j_{\text{DET}+\text{FT}(0.5 \text{ V})} - j_{\text{DET}-\text{FT}(0.5 \text{ V})} \quad (1)$$

$$\Delta j_{\text{MET}} = j_{\text{MET}+\text{FT}(0.5 \text{ V})} - j_{\text{MET}-\text{FT}(0.5 \text{ V})} \quad (2)$$

$\Delta j_{\text{DET}}$  illuminates immediately the ability of the particular AQ derivative to serve as a bridge for DET enzyme voltammetry, and how well the AQ derivatives orient the enzyme on the electrode.  $\Delta j_{\text{MET}}$  reflects the total amount of active enzyme loaded on the electrode irrespective of orientation [3]. The results are further illustrated in Fig. 2A and B. The DET-capable fraction ( $\chi_{\text{DET}\%}$ ) is the percentage of active enzyme oriented

correctly for DET, calculated as the ratio between the two  $\Delta j$ s [3], Eq. (3), Fig. 2C.

$$\chi_{\text{DET}\%} = \frac{\Delta j_{\text{DET}}}{\Delta j_{\text{MET}}} \cdot 100 \quad (3)$$

The results, show, first that both the MET and DET modes are highly sensitive to the electrostatic charge distributions of the Aqs. Although the DET capable fractions,  $\chi_{\text{DET}\%}$  are overall small, a clear dependence on the specific AQ charge distribution is, however, still apparent both in  $\chi_{\text{DET}\%}$  and in enzyme loading. The AQ derivative AQdA (3) offers the most favourable orientation of the enzyme with the largest amount of DET capable enzyme relative to the overall amount of immobilised active FDH. The derivative AQdd (1) allows clearly more enzyme to be bound to the electrode, but in unfavourable orientations (DET low compared to MET). AQSH (4) and AQdS (2) both give low loading of active enzyme, as seen by their  $\Delta j_{\text{MET}}$  values, Fig. 2B. AQSH (4) orients the enzyme in a slightly better DET-favourable orientation compared to AQdS (2), but still in considerably smaller amount than both AQdA (3) and AQdd (1) (Fig. 2A).

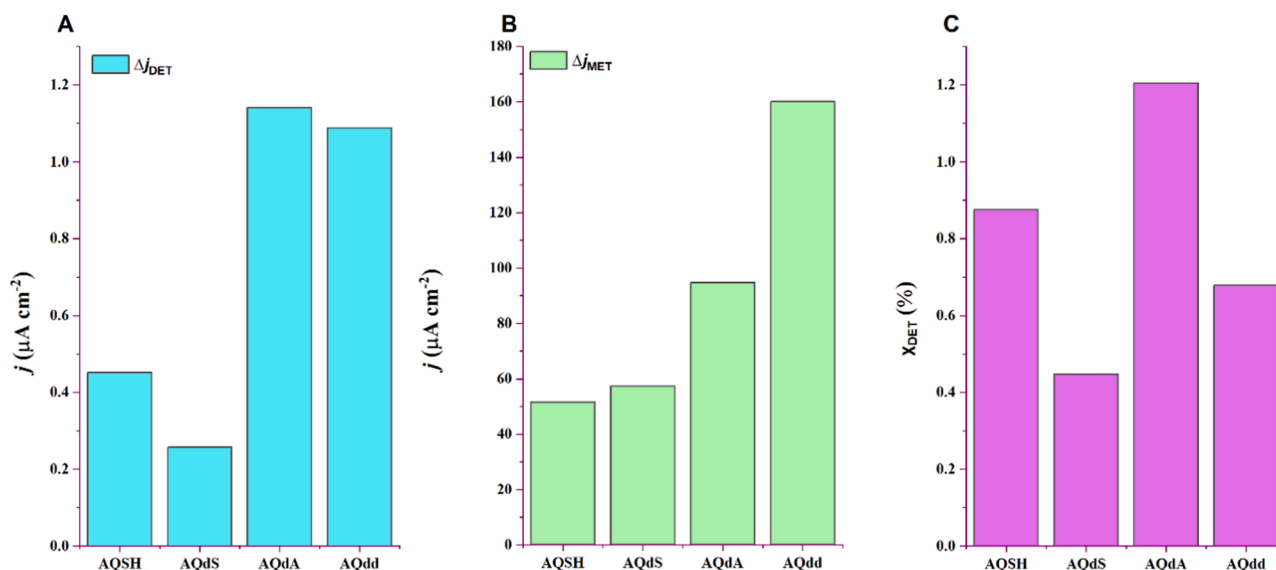


**Fig. 2.** Histograms of the calculated A)  $\Delta j_{\text{DET}}$ , B)  $\Delta j_{\text{MET}}$  and C)  $\chi_{\text{DET}\%}$ .



As noted, the heme 2c group is the end-point for electron relay in the DET process [3,22]. The local FDH surface charge (homology model from [3]) close to the heme 2c group at pH 5.5, Fig. 3 yellow circle, is positive but also with conspicuous hydrophobic areas. This is consistent with AQdA (3) showing the highest  $\chi_{DET\%}$  with the negatively charged sulphonate giving a favourable secondary interaction with the positively charged surface, in addition to the hydrophobic interaction from the anthraquinone core. To summarise, these results verify that strategic chemical design of molecular bridges can affect the orientation of FDH, and that DET as well as MET of FDH is very sensitive to the electrode molecular surface modification.

#### 4. Conclusion

Our study demonstrates the strategic design of anthraquinone-based molecular bridges, guiding the synthesis of four anthraquinones with different functionalities (neutral, anionic or cationic) using a convergent strategy. Starting from 1-ammonio-2-sulphonate substituted AQSH (4), the other three AQs were synthesised by sequential chemoselective substituent removal, yielding 1-amino substituted AQdS (2), 2-sulphonate substituted anthraquinone AQdA (3) and unsubstituted anthraquinone AQdd (1), all of which contain a free thiol group, to form the AQ SAM on Au. Their properties as molecular bridges were analysed, and relevant secondary interactions that align FDH correctly for DET identified.

NPG was chosen as the electrode substrate, as this material has proved both to give high enzyme loadings and to stabilise the immobi-

lized enzyme, with resulting high electrochemical and electrocatalytic currents [3,32,33]. Each electrode was modified with a SAM of a single one of the anthraquinones and then conjugated, through noncovalent, electrostatic and hydrophobic interactions to FDH. Electrochemical analysis of FDH on all the AQ modified NPGs was performed using CV, in the absence or presence of enzyme substrate. Both MET and DET were found to depend strongly on the particular AQ molecular charge distribution. Particularly the calculated  $\chi_{DET\%}$  values for each conjugate indicates that the nature of the anthraquinone substituent has a considerable effect on the AQ ability to orient and interact with the enzyme suitably for efficient DET. The anionic AQdA (3) thus shows the highest DET capable fraction among the four anthraquinones in accordance with the predominantly positively charged surface around the electronic charge inlet heme 2c site.

Our study demonstrates the potential of using carefully designed bridge molecules to align FDH on electrodes in orientations favourable for direct interfacial electrochemical ET. Although the electrochemical mapping of the new surface immobilized AQs points to a clear, largely electrostatically controlled pattern, the DET capable fractions of the overall active enzyme loading  $\chi_{DET\%}$ , however, remain small.  $\chi_{DET\%}$  could be enhanced along three routes. One would be to exploit alkanethiol grafted anthraquinones, as this allows tighter packing of the molecular bridge on the electrode [15]. A second route would exploit further AQ substitution in the AQ frame to fine-tune the AQ equilibrium redox potential. The much lower redox potentials of the AQs ( $E^0$  of ca.  $-0.45$  V vs. Ag/AgCl at pH 5.5) presently addressed compared to the FDH equilibrium potential (that of the FAD cofactor in FDH of  $-0.27$  V

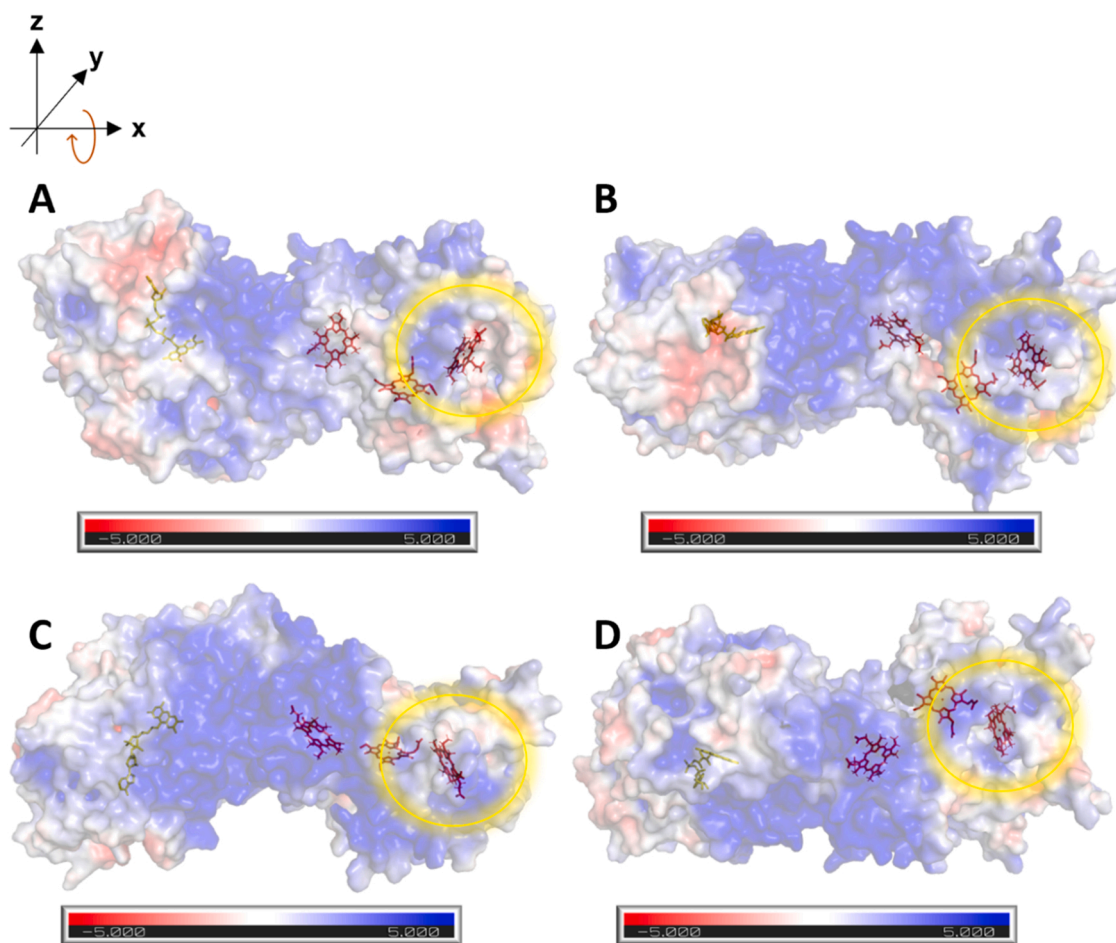


**Fig. 3.** Homology model with surface charge distribution (blue colour indicates the positively charged region, red colour negative charges) at pH 5.5 based on PyMol 2.5 and the PDB2PQR web server [31]. The yellow circle indicates the heme 2c group. From A to B the enzyme is rotated 90 degrees around the x-axis as indicated by the red arrow top left; the same from B to C and from C to D.

at pH 5.5), is thus prohibitive for efficient MET (thermodynamically unfavourable) [30] via immobilized AQ and would also obstruct electron tunnelling (“superexchange” [34,35]) through the AQs due to the high tunnelling barrier. Substitution by electron donating substituents in the AQ frame would thus both raise the AQ redox potentials closer to that of FDH, leading to more favourable MET driving force, and lower the electron tunnelling barrier in DET. Extension to other redox enzymes with redox potentials closer to those of the AQ bridging molecules would be a third approach and offer a wider perspective. Work along these lines is in progress.

### CRedit authorship contribution statement

**Charlotte Uldahl Jansen:** Data curation, Methodology, Writing – original draft. **Xiaomei Yan:** Data curation, Methodology. **Jens Ulstrup:** Conceptualization, Writing – review & editing. **Xinxin Xiao:** Data curation, Conceptualization, Methodology, Writing – review & editing. **Katrine Qvortrup:** Conceptualization, Supervision, Methodology, Writing – review & editing.

### Declaration of Competing Interest

The authors declare that they have no known competing financial interests or personal relationships that could have appeared to influence the work reported in this paper.

### Data Availability

Data will be made available on request.

### Acknowledgments

This work was supported by the grants Carlsberg Foundation Young Researcher Fellowship (grant No. CF18-0631, to K.Q.) and Villum Experiment (Grant No. 35844, to X.X.).

### Appendix A. Supporting information

Supplementary data associated with this article can be found in the online version at doi:10.1016/j.colsurfb.2022.112941.

### References

- [1] V. Hitaishi, et al., Controlling redox enzyme orientation at planar electrodes, *Catalysts* vol. 8 (5) (2018) 192, <https://doi.org/10.3390/catal8050192>.
- [2] I. Mazurenko, V.P. Hitaishi, E. Lojou, Recent advances in surface chemistry of electrodes to promote direct enzymatic bioelectrocatalysis, *Curr. Opin. Electrochem.* vol. 19 (2020) 113–121, <https://doi.org/10.1016/j.coelec.2019.11.004>.
- [3] X. Yan, et al., Direct electron transfer of fructose dehydrogenase immobilized on thiol-gold electrodes, *Electrochim. Acta* vol. 392 (2021), 138946, <https://doi.org/10.1016/j.electacta.2021.138946>.
- [4] N.D.J. Yates, M.A. Fascione, A. Parkin, Methodologies for ‘wiring’ redox proteins/enzymes to electrode surfaces, *Chem. Eur. J.* vol. 24 (47) (2018) 12164–12182, <https://doi.org/10.1002/chem.201800750>.
- [5] J. Lu, M. Nie, Y. Li, H. Zhu, G. Shi, Design of composite nanosupports and applications thereof in enzyme immobilization: a review, *Colloids Surf. B: Biointerfaces* vol. 217 (2022), 112602, <https://doi.org/10.1016/j.colsurfb.2022.112602>.
- [6] J. Bergman, Y. Wang, J. Wigström, A.-S. Cans, Counting the number of enzymes immobilized onto a nanoparticle-coated electrode, *Anal. Bioanal. Chem.* vol. 410 (6) (2018) 1775–1783, <https://doi.org/10.1007/s00216-017-0829-1>.
- [7] J. Alvarez-Malmagro, G. García-Molina, A. López De Lacey, Electrochemical Biosensors Based on Membrane-Bound Enzymes in Biomimetic Configurations, *Sensors* vol. 20 (12) (2020) 3393, <https://doi.org/10.3390/s20123393>.
- [8] X. Xiao, et al., Tackling the challenges of enzymatic (Bio)fuel cells, *Chem. Rev.* vol. 119 (16) (2019) 9509–9558, <https://doi.org/10.1021/acs.chemrev.9b00115>.
- [9] N.R. Mohamad, N.H.C. Marzuki, N.A. Buang, F. Huyop, R.A. Wahab, An overview of technologies for immobilization of enzymes and surface analysis techniques for immobilized enzymes, *Biotechnol. Biotechnol. Equip.* vol. 29 (2) (2015) 205–220, <https://doi.org/10.1080/13102818.2015.1008192>.
- [10] C. Léger, P. Bertrand, Direct electrochemistry of redox enzymes as a tool for mechanistic studies, *Chem. Rev.* vol. 108 (7) (2008) 2379–2438, <https://doi.org/10.1021/cr0680742>.
- [11] P. Bollella, E. Katz, Enzyme-based biosensors: tackling electron transfer issues, *Sensors* vol. 20 (12) (2020) 3517, <https://doi.org/10.3390/s20123517>.
- [12] H.A. Reeve, et al., Enzymes as modular catalysts for redox half-reactions in H<sub>2</sub>-powered chemical synthesis: from biology to technology, *Biochem. J.* vol. 474 (2) (2017) 215–230, <https://doi.org/10.1042/BCJ20160513>.
- [13] D. Leech, P. Kavanagh, W. Schuhmann, Enzymatic fuel cells: Recent progress, *Electrochim. Acta* vol. 84 (2012) 223–234, <https://doi.org/10.1016/j.electacta.2012.02.087>.
- [14] R.D. Milton, S.D. Minter, “Direct enzymatic bioelectrocatalysis: differentiating between myth and reality,” *J. R. Soc. Interface.*, vol. 14, no. 131, p. 20170253, Jun. 2017, doi: 10.1098/rsif.2017.0253.
- [15] A.L. Eckermann, D.J. Feld, J.A. Shaw, T.J. Meade, Electrochemistry of redox-active self-assembled monolayers, *Coord. Chem. Rev.* vol. 254 (15–16) (2010) 1769–1802, <https://doi.org/10.1016/j.ccr.2009.12.023>.
- [16] X. Yan, J. Tang, D. Tanner, J. Ulstrup, X. Xiao, Direct electrochemical enzyme electron transfer on electrodes modified by self-assembled molecular monolayers, *Catalysts* vol. 10 (12) (2020) 1458, <https://doi.org/10.3390/catal10121458>.
- [17] N. Lalaoui, A. LeGoff, M. Holzinger, M. Mermoux, S. Cosnier, Wiring laccase on covalently modified graphene: carbon nanotube assemblies for the direct bioelectrocatalytic reduction of oxygen, *Chem. Eur. J.* vol. 21 (8) (2015) 3198–3201, <https://doi.org/10.1002/chem.201405557>.
- [18] P. Bollella, Y. Hibino, K. Kano, L. Gorton, R. Antiochia, Enhanced direct electron transfer of fructose dehydrogenase rationally immobilized on a 2-aminoanthracene diazonium cation grafted single-walled carbon nanotube based electrode, *ACS Catal.* vol. 8 (11) (2018) 10279–10289, <https://doi.org/10.1021/acscatal.8b02729>.
- [19] T. Adachi, Y. Kaida, Y. Kitazumi, O. Shirai, K. Kano, Bioelectrocatalytic performance of d-fructose dehydrogenase, *Bioelectrochemistry* vol. 129 (2019) 1–9, <https://doi.org/10.1016/j.bioelechem.2019.04.024>.
- [20] Y. Hibino, S. Kawai, Y. Kitazumi, O. Shirai, K. Kano, Mutation of heme c axial ligands in d-fructose dehydrogenase for investigation of electron transfer pathways and reduction of overpotential in direct electron transfer-type bioelectrocatalysis, *Electrochem. Commun.* vol. 67 (2016) 43–46, <https://doi.org/10.1016/j.elecom.2016.03.013>.
- [21] C.U. Jansen, “A Novel Site-Selective Bioconjugation Strategy for the Synthesis of Energy Harvesting Protein-Conjugates,” PhD Thesis, Technical University of Denmark, 2022.
- [22] S. Kawai, T. Yakushi, K. Matsushita, Y. Kitazumi, O. Shirai, K. Kano, The electron transfer pathway in direct electrochemical communication of fructose dehydrogenase with electrodes, *Electrochem. Commun.* vol. 38 (2014) 28–31, <https://doi.org/10.1016/j.elecom.2013.10.024>.
- [23] J. Clayden, N. Greeves, S.G. Warren, *Organic Chemistry, second ed.*, Oxford University Press, Oxford; New York, 2012.
- [24] J.P. Guthrie, Hydrolysis of esters of oxy acids:  $pK_a$  values for strong acids; Brønsted relationship for attack of water at methyl; free energies of hydrolysis of esters of oxy acids; and a linear relationship between free energy of hydrolysis and  $pK_a$  holding over a range of 20  $pK$  units, *Can. J. Chem.* vol. 56 (17) (1978) 2342–2354, <https://doi.org/10.1139/v78-385>.
- [25] Y. Baqi, C.E. Müller, Rapid and efficient microwave-assisted copper(0)-catalyzed ullmann coupling reaction: general access to anilinoanthraquinone derivatives, *Org. Lett.* vol. 9 (7) (2007) 1271–1274, <https://doi.org/10.1021/ol070102v>.
- [26] Y. Baqi, C.E. Müller, Efficient and mild deamination procedure for 1-aminoanthraquinones yielding a diverse library of novel derivatives with potential biological activity, *Tetrahedron Lett.* vol. 53 (50) (2012) 6739–6742, <https://doi.org/10.1016/j.tetlet.2012.09.011>.
- [27] C. Cremer, O. Wallquist, “Sulfide dyes,” WO2006136516A2.
- [28] M. Peng, E. Du, Z. Li, D. Li, H. Li, Transformation and toxicity assessment of two UV filters using UV/H<sub>2</sub>O<sub>2</sub> process, *Sci. Total Environ.* vol. 603–604 (2017) 361–369, <https://doi.org/10.1016/j.scitotenv.2017.06.059>.
- [29] X. Xiao, J. Ulstrup, H. Li, M. Wang, J. Zhang, P. Si, Nanoporous gold assembly of glucose oxidase for electrochemical biosensing, *Electrochim. Acta* vol. 130 (2014) 559–567, <https://doi.org/10.1016/j.electacta.2014.02.146>.
- [30] X. Yan, et al., Surface-confined redox-active monolayers of a multifunctional anthraquinone derivative on nanoporous and single-crystal gold electrodes, *Electrochem. Commun.* vol. 124 (2021), 106962, <https://doi.org/10.1016/j.elecom.2021.106962>.
- [31] E. Jurrus, et al., Improvements to the APBS biomolecular solvation software suite, *Protein Sci.* vol. 27 (1) (2018) 112–128, <https://doi.org/10.1002/pro.3280>.
- [32] T. Siepenkoetter, et al., Immobilization of redox enzymes on nanoporous gold electrodes: applications in biofuel cells, *ChemPlusChem* vol. 82 (4) (2017) 553–560, <https://doi.org/10.1002/cplu.201600455>.
- [33] X. Xiao, P.O. Conghaile, D. Leech, R. Ludwig, E. Magner, A symmetric supercapacitor/biofuel cell hybrid device based on enzyme-modified nanoporous gold: An autonomous pulse generator, *Biosens. Bioelectron.* vol. 90 (2017) 96–102, <https://doi.org/10.1016/j.bios.2016.11.012>.
- [34] A.M. Kuznefsov, J. Ulstrup, *Electron transfer in chemistry and biology: an introduction to the theory*, John Wiley & Sons Ltd, Chichester, 1999.
- [35] R.R. Nazmutdinov, J. Ulstrup, “Retrospective and Prospective Views of Electrochemical Electron Transfer Processes: Theory and Computations,” in *Atomic-Scale Modelling of Electrochemical Systems*, 1st ed., M. M. Melander, T. T. Laurila, and K. Laasonen, Eds. Wiley, 2021, pp. 25–91. doi: 10.1002/9781119605652.ch2.